PHYSICS AND CHEMISTRY OF SOLID STATE
V. 27, No. 1 (2026) pp. 144-151
Section: Physics

DOI: 10.15330/pcss.27.1.144-151

Vasyl Stefanyk Carpathian National University

ФІЗИКА І ХІМІЯ ТВЕРДОГО ТІЛА
Т. 27, № 1 (2026) С. 144-151
Фізико-математичні науки

PACS: 79.20.Eb, 61.80.Ba, 42.62.Cf

ISSN 1729-4428 (Print)
ISSN 2309-8589 (Online)

I. Shtablavyi, Yu. Kulyk, A. Pauk, N. Popilovskyi, M. Yatsevych, S. Mudry

Selective laser melting of Al-Cu-Fe based alloys using elemental powder blends

Department of Metal Physics, Ivan Franko National University of Lviv, Lviv, Ukraine; ihor.shtablavyi@lnu.edu.ua

In this work, the conditions for obtaining the $Al_{63}Cu_{25}Fe_{12}$ alloy from a mixture of elemental powders by selective laser melting were investigated. In addition to directly synthesizing the alloy using the mentioned method, the aim of this work was also to identify the conditions for the formation of quasi-crystalline phases, which have special mechanical properties. Selective laser melting was performed at different powers and geometries of laser irradiation in air and in vacuum. Scanning electron microscopy and X-ray phase analysis methods were used to study the prepared alloys. It has been shown that, in addition to the generally accepted modes of laser alloy synthesis, focusing the laser beam on the surface of the samples plays an important role in this process.

Keywords: additive manufacturing, selective laser melting, aluminium alloys, quasicrystals, electron microscopy.

Received 14 November 2025; Accepted 05 February 2026; Published 26 March 2026.

Introduction

3D metal printing technologies are extremely promising for replacing traditional manufacturing methods. Among them, laser sintering or melting of metal powders are at the forefront. In this case, powders with a composition corresponding to the required alloy are used to form three-dimensional objects. Quite often, additional requirements are imposed on the powders used, relating to their geometry and elemental composition, which makes them significantly more expensive. In view of this, studies related to the use of elemental powders in laser 3D printing to form bulk objects based on the required alloys is a top priority.

Currently, there are studies related to the technology of 3D printing of metal alloys using elemental powders [1, 2]. These works mainly concern the production of simple alloys and intermetallic compounds, and the results obtained in them have limited application. Despite the limited applicability of the alloys obtained in these works, certain important conclusions can still be drawn from them. In particular, work [1] showed that the use of elemental aluminum and silicon powders for the synthesis of eutectic alloys results in the brittleness of the resulting alloy compared to the use of eutectic composition powder. The reason for this is obviously the significant difference in the melting temperatures of the components, which affects the degree of alloying of aluminum and silicon powders. On the other hand, it was shown in paper [2] that it's possible to obtain high-quality aluminum-based alloys with refractory metals scandium and zirconium. In this case, intermetallic compounds are formed in alloys, which increase the hardness of them. The possibility of forming alloys by selective laser melting of non-spherical elemental powders has also been demonstrated for the Ti-Nb system [3]. As a result of the research conducted in this work, it was established that the amount of irradiation energy strongly affects the porosity and homogeneity of the obtained alloys. The analyzed studies show that the selective laser melting method can be used to obtain homogeneous alloys from elemental powders of non-spherical shape in the case where it is difficult to synthesize powders of the required composition.

Aluminum-based alloys are lightweight alloys with excellent corrosion resistance properties. The addition of refractory metals to aluminum causes the formation of highly dispersed phases that can strengthen the alloy without reducing other properties. For example, addition

of iron and copper causes the formation of quasi-crystalline phases. In general, the phase diagram of Al-Cu-Fe ternary alloys is well studied [4-6] due to the wide practical application of them. As a result of these studies, it was established that at a temperature of 700 °C, the interval of existence of the icosahedral phase is $Al_{67-56}Cu_{24-31}Fe_{9-13}$ and decreases to $Al_{66-58}Cu_{23-28}Fe_{11-14}$ when the temperature rises to 800 °C. In addition, the process of Al-Cu-Fe alloys crystallization by electromagnetic levitation was studied in detail [7], and the sequence of phase formation in them was analyzed [8, 9].

The highest interest in Al-Cu-Fe alloys is due to their mechanical [10, 11] and corrosion resistance [12] properties. In particular, four alloys were studied in [10], namely $Al_{65}Cu_{20}Fe_{15}$, $Al_{64}Cu_{22.5}Fe_{13.5}$, $Al_{61}Cu_{26}Fe_{13}$ and $Al_{62}Cu_{25.5}Fe_{12.5}$ and their phase composition and mechanical properties were analyzed. These alloys were studied in both as-cast state and after heat treatment. It was shown that the first two alloys contained the highest amount of λ-$Al_{13}Fe_4$ phase and exhibited the highest hardness. The other two alloys are more easily heat treated. Many other works concern the production of alloys and composites of this system by mechanical alloying and subsequent compaction [13-15]. A common feature of these works is that the production of alloys, especially composites based on aluminum and quasi-crystalline phases, by powder metallurgy has the potential for practical implementation and application.

Currently, selective laser melting of powder is used to synthesize alloys of the Al-Cu-Fe system [16-18]. These works investigate the phase composition, microstructure, and mechanical properties of Al–2.5Fe–2Cu (mass%) alloys after laser melting and as a result of annealing after synthesis. In [16], studies were performed on the relationship between the microstructure of alloys and their mechanical properties. It has been shown that the formation of the $Al_{23}CuFe_4$ phase contributes to the improvement of the mechanical properties of the alloy. It also indicates low thermal conductivity of the alloy after laser melting [17], although after annealing, thermal conductivity increases without loss of strength. In addition to these studies, it is worth mentioning works related to the production of porous alloys based on the Al-Cu-Fe system [19, 20].

Taking into account the information mentioned above, Al-Cu-Fe alloys are popular due to their physical and chemical properties. However, there is limited information on the synthesis of these alloys by selective laser melting from elemental powders. Therefore, in this work, we studied the conditions for obtaining ternary $Al_{63}Cu_{25}Fe_{12}$ alloy by selective laser melting under different processing modes. The main focus was made on the conditions for the formation of homogeneous and non-porous alloys with quasi-crystalline phases.

I. Experimental

A mixture of aluminum, copper, and iron powders was used as the raw material for synthesis. We have studied the $Al_{63}Cu_{25}Fe_{12}$ alloy in which, according to [21], the highest fraction of quasi-crystalline phase is formed.

For alloy synthesis, we used a Ytterbium-doped pulsed fiber laser with a wavelength of 1064 nm and a maximum optical power of 50 W. Laser treatment was performed at a beam power of 20 to 45 W and a scanning speed of 1000 mm/s. The amount and geometry of absorbed energy were controlled by displacing the laser focus above the sample (displaced focus − modes 1-3). For maximum energy absorption per unit area of the sample, the laser beam was focused (mode 4). Details about laser scanning modes are provided in Table 1.

Table 1.

Modes of laser alloy synthesis.

Mode number	Laser power, W	Scanning speed, mm/s	Focus
1	20	1000	displaced
2	40	1000	displaced
3	45	1000	displaced
4	45	1000	pointed

The resulting alloys were studied using scanning electron microscopy and X-ray phase analysis.

X-ray diffraction (XRD) analysis of alloys was carried out using a STOE STADI P powder diffractometer, equipped with a linear position-sensitive detector (PSD) in a modified Guinier geometry setup in Bragg-Brentano transmission mode. Measurement conditions were as follows: monochromatic Cu $K_{\alpha 1}$ radiation (λ = 1.540598 Å); bent Johannson-type [111] Ge monochromator; ω/2θ scan; 2θ range of 4° to 120°; step size of 0.480° (2θ); step scan time of 60 seconds per data point.

For the investigations of the microstructure of alloys a field emission scanning electron microscopy (FESEM) analysis was performed using a Hitachi S-4100 microscope with a secondary electron detector. The scanning of the sample surface was carried out by electron beam operating at 15 kV and 10 μA with the spatial resolution of 10 nm in the secondary electron image regime.

II. Results and discussion.

The synthesis of alloys from powders began with preliminary melting and removal of absorbed gases from the powder volume under mode 1 with a fivefold scanning. The main melting procedure was carried out in accordance with modes 2 or 3. Melting in accordance with this method was carried out in an air atmosphere. The synthesis of alloys was also carried out in a vacuum in accordance with modes 1, 2, 3, and 4. The latter mode was used to increase the absorbed energy density and ensure uniform melting of alloys. After synthesis, the alloys were examined using electron microscopy and X-ray analysis.

Figure 1 shows the results of the surface morphology study of $Al_{63}Cu_{25}Fe_{12}$ alloys obtained by selective laser melting in air at a scanning distance of 60 micrometers and different irradiation energies. As we can see, in the case of minimal irradiation energy, aluminum, copper, and iron microparticles are only partially connected to each other, indicating incomplete melting and fusion between them (Fig. 1, a). Analysis of individual alloy regions indicates

the presence of nanoscale spheres or hemispheres (Fig. 1,b), which were probably formed as a result of intense metal ablation and subsequent deposition on the alloy surface. As can be seen from these figures, the mechanical properties of the obtained alloys are quite low due to the significant porosity of the sample.

Increasing the laser radiation power from 40 to 45 W does not markedly improve densification, although localized nanostructures such as nanoneedles appear on the surface, and, as in the previous case, the melt solidifies into a porous structure. Analysis of the individual characteristics of the alloyed regions revealed the presence of areas of intense alloy evaporation, resulting in the formation of nanoneedles approximately one micrometer long and less than one hundred nanometers in diameter after deposition (Fig. 1 c, d). As can be seen in Figure 1,c, these nanoneedles are formed outside the craters of the most intense evaporation of material.

Reducing the distance between laser scanning tracks to 30 micrometers under the same irradiation conditions significantly affects the degree of alloy porosity, reducing it (Fig. 2). In particular, although the particles of the alloy surface are not completely melted, their satisfactory consolidation is observed. This effect is likely caused by an increase in the energy density absorbed by the alloy and less dissipation into the environment.

An important feature of the alloy surface melted under modes 1-2 is the formation of a quasi-grained structure (Fig. 2,a). Analysis of the individual features of the surface formation of the alloyed areas, as in the case of a scanning step of 60 micrometers, indicates the formation of spherical structures resulting from the intense evaporation of the molten areas.

Increasing the maximum irradiation power to 45 W leads to the formation of larger areas of alloyed material compared to previous cases. Analysis of the microstructure of these areas indicates the formation of grains approximately 60 micrometers in size, which is comparable to the size of the original powder particles (Fig. 2, c). As it was found out by microscopic analysis, the surface of such grains is nanostructured with regularly arranged cylindrical crystallites.

Phase analysis of the alloys was carried out using X-ray phase analysis (Fig. 3). It was found that the alloys do not contain pure components from which they were synthesized, and therefore they have completely reacted with each other. As a result of alloy crystallization under various irradiation conditions, Al_2Cu and $Al_{13}Fe_4$ compounds are formed, as well as a quasi-crystalline ψ-phase. It is also important that no metal oxides were detected, despite the fact that the synthesis was carried out in an air atmosphere.

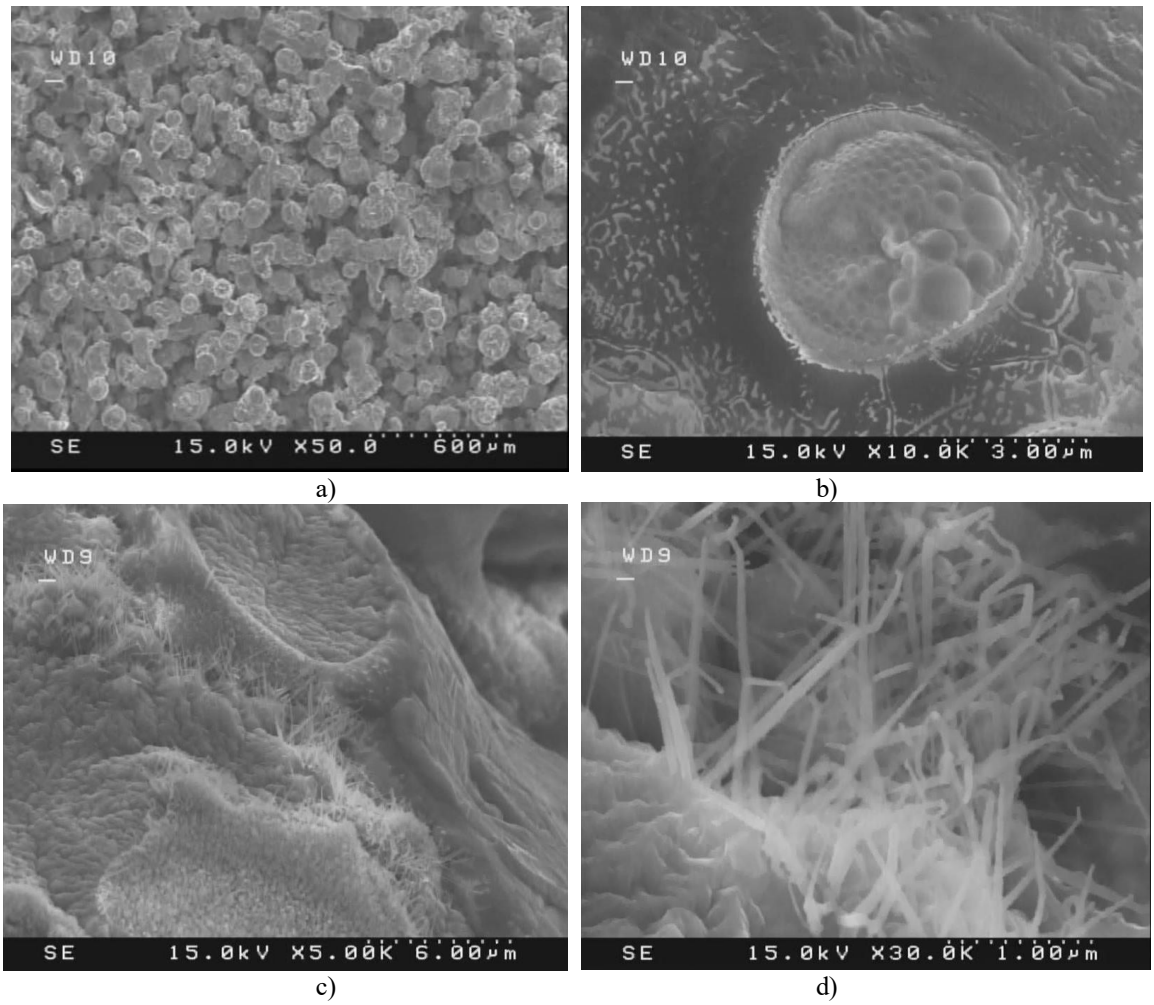

Fig. 1. Microstructure of $Al_{63}Cu_{25}Fe_{12}$ alloys obtained under modes 1-2 (a, b) and 1-3 (c, d) in air with a hatch spacing of 60 μm between scan tracks.

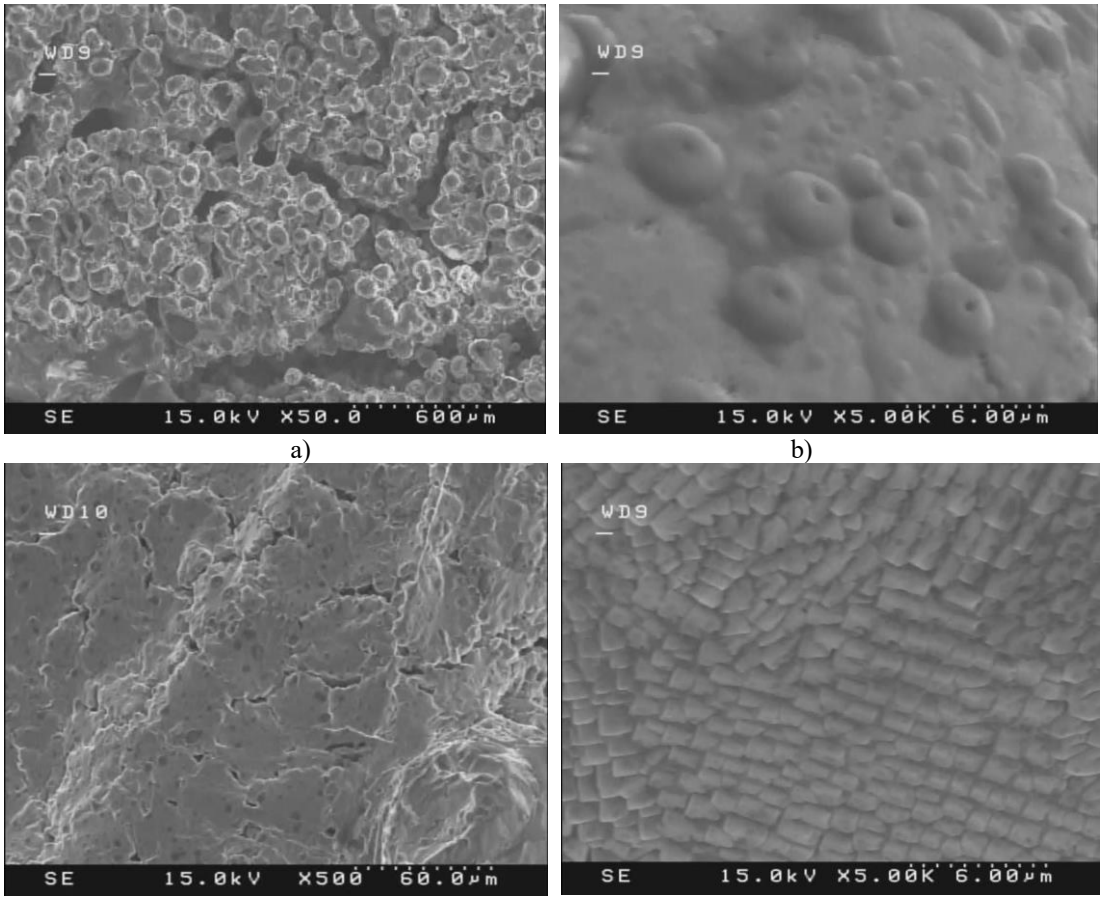

Fig. 2. Microstructure of $Al_{63}Cu_{25}Fe_{12}$ alloys obtained under modes 1-2 (a, b) and 1-3 (c, d) in air with a hatch spacing of 30 µm between scan tracks.

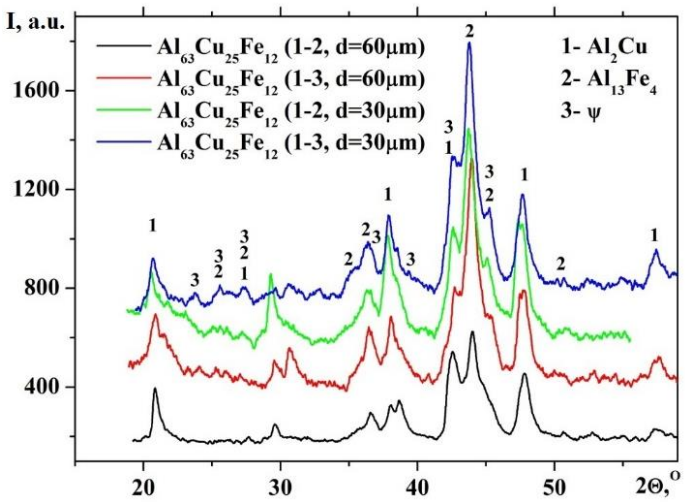

Fig. 3. Results of phase analysis of $Al_{63}Cu_{25}Fe_{12}$ alloys obtained by laser melting under different conditions in air.

The $Al_{63}Cu_{25}Fe_{12}$ alloy was obtained by selective laser melting, also in a vacuum, under the same conditions as in air, with a scanning distance of 30 micrometers. As in the case of alloy synthesis in air under scanning modes 1-2, incomplete alloying of particles occurs, although the degree of alloying is better compared to the previous case. Under melting regime 1-3, larger alloy areas are formed, and a more detailed study of the microstructure of these areas has revealed dendritic crystallization of the alloy (Fig. 4, b).

The most efficient mode of laser powder melting was found to be one in which, after sintering at a power of 45 W and defocused irradiation, the laser beam was focused and the sample was irradiated again at a power of 45 W. In this case, the particles are completely fused and the surface of the alloy becomes smooth (Fig. 4, c,d). This result is caused by the higher density of absorbed energy per unit area of the alloy. A more detailed analysis of the microstructure revealed a polycrystalline structure of the alloys with grain sizes of about 30-40 micrometers. The grain surfaces were found to exhibit nanoscale roughness.

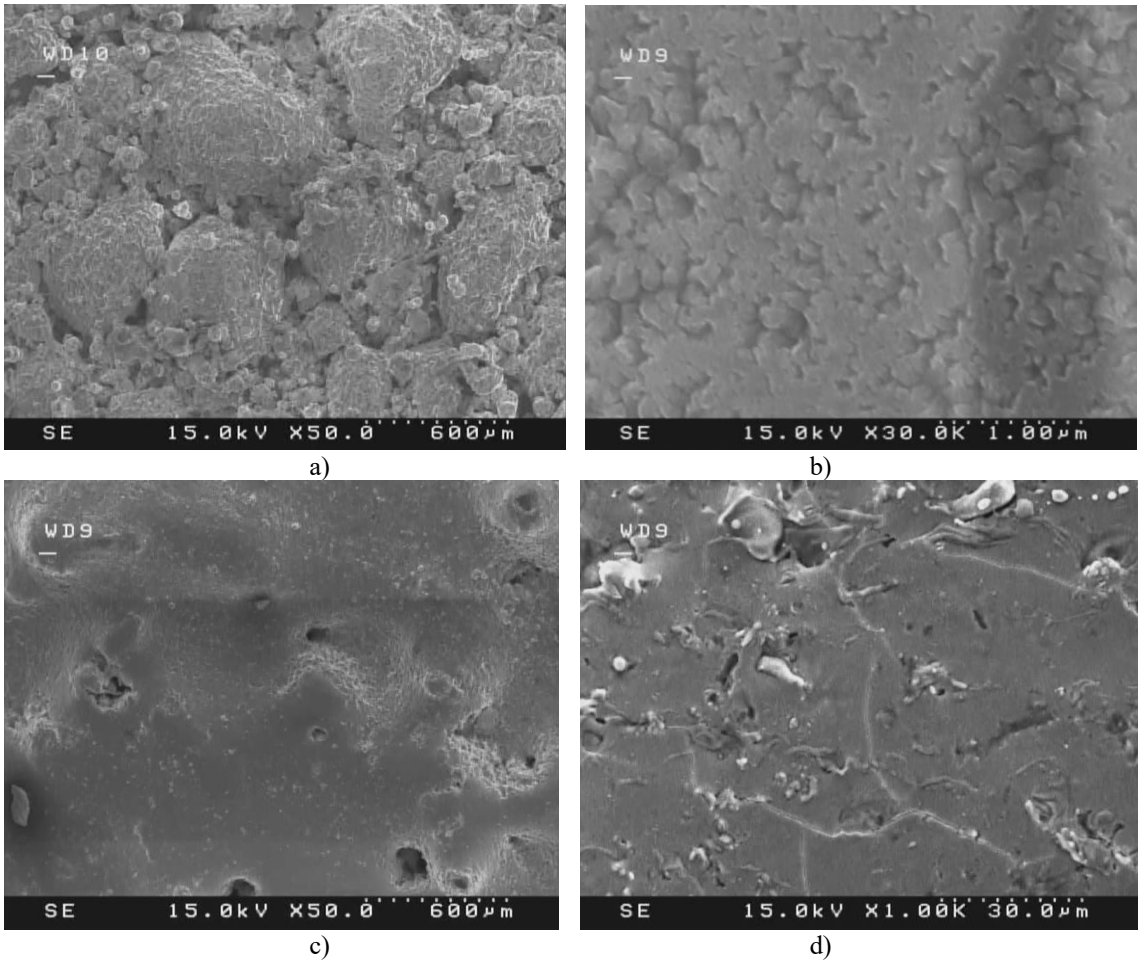

Fig. 4. Microstructure of $Al_{63}Cu_{25}Fe_{12}$ alloys obtained under modes 1–3 (a,b) and sequentially under modes 1–3 followed by mode 4 (c,d) in a vacuum with a hatch spacing of 30 µm.

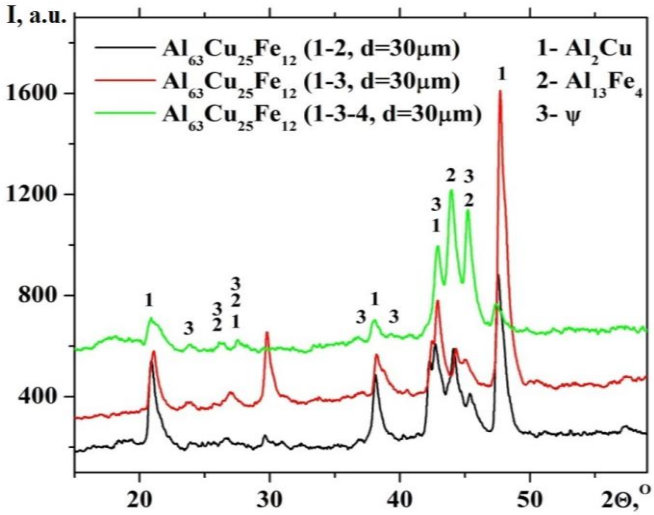

Fig. 5. Phase analysis results for $Al_{63}Cu_{25}Fe_{12}$ alloys obtained by laser melting under various conditions in vacuum.

The results of X-ray phase analysis indicate the absence of separate phases of aluminum, copper, and iron, which indicates their complete fusion and the formation of binary phases Al_2Cu, $Al_{13}Fe_4$, as well as a quasi-crystalline ψ-phase. The increase in the relative intensity of diffraction peaks corresponding to the quasi-crystalline ψ-phase indicates a higher fraction of this phase with increasing absorbed energy density. However, even at minimum radiation energy, a small amount of the quasi-crystalline ψ-phase is present in the alloys.

For quantitative evaluation of the melting result of the metal powder blend, we obtained size distribution functions (Fig 6 a,b) of microobjects shown in Figures 1, 2, and 4. Figure 6a shows the distribution of spheres obtained as a result of laser processing at low absorbed energy values (mode 1-2 in Table 1) at different distances between laser scanning lines (hatching distance). As we can see, the most probable sizes of spherical inclusions are close to 60-70 µm and decrease as the hatching distance decreases.

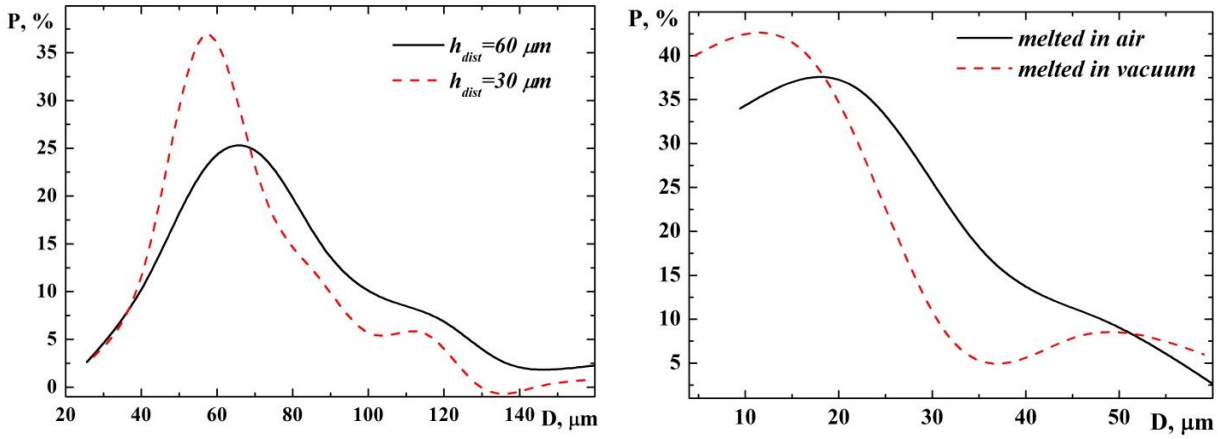

a) b)

Fig. 6. Particle size distribution functions after their alloying under different laser processing modes.

Increasing the irradiation energy leads to a radical change in the surface morphology and, accordingly, in the distribution of surface inhomogeneities by size (Fig. 6, b). In this case, in addition to large baked areas of about 50 μm, there are particles much smaller than the size of the powder used for alloy synthesis. The latter may be caused by splashing of the melt during laser scanning.

The formation of such microscopic spherical surface inhomogeneities occurs due to incomplete melting of particles under conditions of low absorbed radiation energy. Similar results were obtained for magnesium- and aluminium-based alloys [22, 23]. These works indicate several reasons for the formation of spherical structures associated with low melt temperature. These include the presence of an aluminum oxide film, high scanning speed, poor wetting, and capillary/thermal instabilities (Plateau–Rayleigh).

Taking into account the possible factors affecting the surface morphology of the obtained alloys, we changed the mode of its final laser treatment. It should be noted that for preliminary melting, we used processing modes with low energy impact on the alloy that, in addition to changing the irradiation power, was accompanied by placing the sample below the laser beam focusing plane. To increase the absorbed energy density in the case of final processing, the sample surface was placed in the laser focal plane. As a result, a smooth alloy surface with the required phase composition was obtained (Fig. 4 c,d).

Conclusions.

Alloys with the composition of $Al_{63}Cu_{25}Fe_{12}$ were obtained by selective laser melting from elemental powders as precursors. The study of the microstructure of alloys obtained under different irradiation conditions made it possible to establish the optimal conditions under which the alloy exhibited desired structural characteristics.

It has been assumed that surface defects in the form of spherical inclusions arise due to low energy absorption by the alloy, accompanied by poor mutual wetting of molten particles and capillary and thermal instability.

The results of phase analysis showed the absence of metal oxides on the surface of the alloys after laser melting in air. X-ray phase analysis allowed us to establish the presence of Al_2Cu, $Al_{13}Fe_4$ phases, as well as a quasi-crystalline ψ-phase in the obtained alloys. X-ray phase analysis showed that the quasi-crystalline phase occurs both in the case of laser melting in air and in vacuum.

An important outcome of this work is the demonstration that the selective laser melting method enables the fabrication of bulk Al–Cu–Fe alloys with quasicrystalline phases directly from elemental powder blends.

Acknowledgments

This work was supported by the National Research Foundation of Ukraine (Project No 2025.06/0016).

Shtablavyi Ihor − Doctor of Physical and Mathematical Sciences, Professor;
Kulyk Yuriy − Candidate of Physical and Mathematical Sciences (Ph.D.), Senior Researcher;
Pauk Andriy − PhD Student;
Popilovskyi Nazar − Ph.D.;
Yatsevych Maryna – *Master student;*
Mudry Stepan − Doctor of Physical and Mathematical Sciences, Professor, Head of department.

[1] N. Kang, P. Coddet, L Dembinski, H. Liao, Ch. Coddet, *Microstructure and strength analysis of eutectic Al-Si alloy in-situ manufactured using selective laser melting from elemental powder mixture*, Journal of Alloys and Compounds, 691, 316 (2017); https://doi.org/10.1016/j.jallcom.2016.08.249.

[2] J. A Glerum, Ch. Kenel, T. Sun, D. C. Dunand, *Synthesis of precipitation-strengthened Al-Sc, Al-Zr and Al-Sc-Zr alloys via selective laser melting of elemental powder blends*, Additive Manufacturing, 36, 101461 (2020); https://doi.org/10.1016/j.addma.2020.101461.

[3] M. Fischer, D. Joguet, G. Robin, L. Peltier, P. Laheurte. *In situ elaboration of a binary Ti–26Nb alloy by selective laser melting of elemental titanium and niobium mixed powders*, Materials Science and Engineering: C, 62, 852 (2016); https://doi.org/10.1016/j.msec.2016.02.033.

[4] V. Raghavan, *Al-Cu-Fe (Aluminum-Copper-Iron*), Journal of Phase Equilibria and Diffusion, 26, 59 (2005); https://doi.org/10.1007/s11669-005-0061-0.

[5] Lilong Zhu, Sujeily Soto-Medina, Wesley Cuadrado-Castillo, Richard G. Hennig, Michele V. Manuel, *New experimental studies on the phase diagram of the Al-Cu-Fe quasicrystal-forming system*, Materials & Design, 185, 108186 (2019); https://doi.org/10.1016/j.matdes.2019.108186.

[6] Hai-Lin Chen, Yong Du, Honghui Xu, and Wei Xiong, *Experimental investigation and thermodynamic modeling of the ternary Al–Cu–Fe system,* J. Mater. Res., 24 (10), 3154 (2009); https://doi.org/10.1557/JMR.2009.0376.

[7] D. Holland-moritz, J. Schroers, D. M. Herlach, B. Grushko and K. Urban, *Undercooling and solidification behaviour of melts of the quasicrystal-forming alloys Al–Cu–Fe and Al–Cu–Co,* Acta mater, 46 (5), 1601 (1998); https://doi.org/10.1016/s1359-6454(97)00341-8.

[8] S.M. Lee, H.J. Jeon, B.H. Kim, W.T. Kim, D.H. Kim, *Solidification sequence of the icosahedral quasicrystal forming Al–Cu–Fe alloys,* Materials Science and Engineering A, 304–306, 871 (2001); https://doi.org/10.1016/S0921-5093(00)01625-7.

[9] Felipe Escher Saldanha, Jaderson Rodrigo da Silva Leal, Jos´e Eduardo Spinelli, Guilherme Lisboa de Gouveia, *Microstructural evolution and intermetallic formation in as-cast Al-5 % Cu-1.2 %Fe and Al-5 %Cu-1.2 %Fe-1 %Ni: A solidification path variation induced by Ni,* Journal of Alloys and Compounds, 1039, 183280 (2025); https://doi.org/10.1016/j.jallcom.2025.183280.

[10] M.A. Suárez, R. Esquivel, J. Alcántara, H. Dorantes, J.F. Chávez, *Effect of chemical composition on the microstructure and hardness of Al–Cu–Fe alloy,* Materials Characterization, 62, 917 (2011); https://doi.org/10.1016/j.matchar.2011.06.009.

[11] A. Školáková, P. Novák, L. Mejzlíková, F. Pruša, P. Salvetr and D. Vojtech, *Structure and Mechanical Properties of Al-Cu-Fe-X Alloys with Excellent Thermal Stability,* Materials, 10(11), 1269 (2017); https://doi.org/10.3390/ma10111269.

[12] R. Babilasa, A, Bajorek, M. Spilka, A. Radoń, W. Łoński. *Structure and corrosion resistance of Al–Cu–Fe alloys*, Progress in Natural Science: Materials International, 30, 393 (2020); https://doi.org/10.1016/j.pnsc.2020.06.002.

[13] F. Schurack, J, Eckert and L, Schultz, *Synthesis and mechanical properties of mechanically alloyed Al–Cu–Fe quasicrystalline composites*, Philosophical Magazine, 83(11), 1287 (2003); https://doi.org/10.1080/1478643031000076613.

[14] F. Tang, I.E. Anderson, S.B. Biner, *Microstructures and mechanical properties of pure Al matrix composites reinforced by Al–Cu–Fe alloy particles*, Materials Science and Engineering A, 363, 20 (2003); https://doi.org/10.1016/S0921-5093(03)00433-7.

[15] G. Laplanche, A. Joulain, J. Bonneville, R. Schaller, T. El Kabir, *Microstructures and mechanical properties of Al-base composite materials reinforced by Al–Cu–Fe particles*, Journal of Alloys and Compounds, 493, 453 (2010); https://doi.org/10.1016/j.jallcom.2009.12.124.

[16] Yue Cheng, Takanobu Miyawaki, Wenyuan Wang, Naoki Takata, Asuka Suzuki, Makoto Kobashi, Masaki Kato, *Variation in microstructural features of melt-pool structure in laser powder bed fused Al–Fe–Cu alloy at elevated temperatures*, Journal of Materials Research and Technology, 32, 4048 (2024); https://doi.org/10.1016/j.jmrt.2024.09.013.

[17] Yue Cheng, Takanobu Miyawaki, Wenyuan Wang, Naoki Takata, Asuka Suzuki, Makoto Kobashi, Masaki Kato, *Laser-beam powder bed fusion of Al–Fe–Cu alloy to achieve high strength and thermal conductivity*, Additive Manufacturing Letters, 8, 100191 (2024); https://doi.org/10.1016/j.addlet.2023.100191.

[18] Y Cheng, Y Otani, N Takata, A Suzuki, M Kobashi and M Kato, *Inhomogeneous deformation in melt-pool structure of AlFe-Cu alloy manufactured by laser powder bed fusion,* IOP Conf. Series: Materials Science and Engineering, 1310, 012016 (2024); https://doi.org/10.1088/1757-899X/1310/1/012016.

[19] J. M. Hernández, I. A. Figueroa, G. González, A. E. Salas, L. E. Mendoza, I. Alfonso, G. A. Lara-Rodríguez, *In-situ porosity formation of self-foaming Al-Fe-Cu alloys*, Applied Physics A, 128, 319 (2022); https://doi.org/10.1007/s00339-022-05454-8.

[20] M.A. Suarez, M.F. Delgado-Pamanes, J.F. Chavez-Alcal, A. Cruz-Ramírez, I. Guadarrama, I.A. Figueroa, *Microstructural and mechanical characterization of quasicrystalline Al-Cu-Fe foams*, Materials Today Communications, 30, 103043 (2022); https://doi.org/10.1016/j.mtcomm.2021.103043.

[21] O. V. Sukhova, V. A. Polonskyy, K. V. Ustinova, M. V. Berun, *Corrosion behaviour of quasicrystal Al – Cu – Fe and Al – Ni – Fe alloys in acidic solutions,* The Scientific Technical journal Metal Science and Treatment of Metals, 24(4). 19, (2018); https://momjournal.org.ua/index.php/mom/article/view/2018-4-3/2018-4-3.

[22] Shuai Liu and Hanjie Guo, *Balling Behavior of Selective Laser Melting (SLM) Magnesium Alloy*, Materials, 13, 3632 (2020); https://doi.org/10.3390/ma13163632.

[23] N.T. Aboulkhair, M. Simonelli, L. Parry, I. Ashcroft, Ch. Tuck, R. Hague, *3D printing of Aluminium alloys: Additive Manufacturing of Aluminium alloys using selective laser melting,* Progress in Materials Science, 106, 100578 (2019); https://doi.org/10.1016/j.pmatsci.2019.100578.

І. Штаблавий, Ю. Кулик, А. Паук, Н. Попільовський, М. Яцевич, С. Мудрий

Селективне лазерне плавлення сплавів на основі Al-Cu-Fe з використанням сумішей елементарних порошків

Кафедра фізики металів, Львівський національний університет імені Івана Франка, Львів, Україна,
ihor.shtablavyi@lnu.edu.ua,

У цій роботі досліджено умови отримання сплаву $Al_{63}Cu_{25}Fe_{12}$ із суміші елементарних порошків методом селективного лазерного плавлення. Окрім безпосереднього синтезу сплаву зазначеним методом, метою роботи було також визначення умов утворення квазікристалічних фаз, які мають особливі механічні властивості. Селективне лазерне плавлення проводили при різних потужностях і геометрії лазерного опромінення в повітрі та у вакуумі. Для дослідження отриманих сплавів використовували методи скануючої електронної мікроскопії та рентгенівського фазового аналізу. Показано, що, крім загальноприйнятих режимів лазерного синтезу сплавів, важливу роль у цьому процесі відіграє фокусування лазерного променя на поверхні зразків.

Ключові слова: адитивне виробництво, селективне лазерне плавлення, алюмінієві сплави, квазікристали, електронна мікроскопія.